

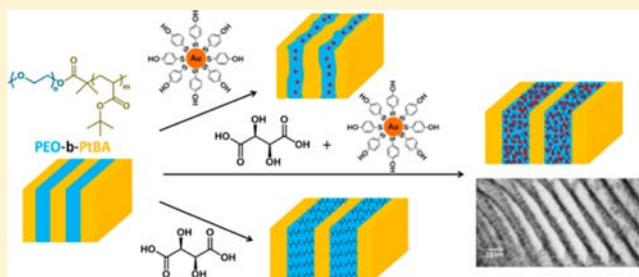
Ultrahigh Loading of Nanoparticles into Ordered Block Copolymer Composites

Li Yao, Ying Lin, and James J. Watkins*

Department of Polymer Science and Engineering, University of Massachusetts Amherst, 120 Governors Drive, Amherst, Massachusetts 01003, United States

Supporting Information

ABSTRACT: Phase selective, ultrahigh loading of nanoparticles into target domains of block copolymer composites was achieved by blending the block copolymer hosts with small molecule additives that exhibit strong interactions with one of the polymer chain segments and with the nanoparticle ligands via hydrogen bonding. The addition of D-tartaric acid to poly(ethylene oxide-*block*-*tert*-butyl acrylate) (PEO-*b*-PtBA) enabled the loading of more than 150 wt % of 4-hydroxythiophenol-functionalized Au nanoparticles relative to the mass of the target domain (PEO + tartaric acid), which corresponds to greater than 40 wt % Au by mass of the resulting well-ordered composite as measured by thermal gravimetric analysis. The additive, tartaric acid, performs three important roles. First, as evidenced by small-angle X-ray scattering, it significantly increases the segregation strength of the block copolymer via selective interaction with the hydrophilic PEO block. Second, it expands the PEO block and enhances the number and strength of enthalpically favorable interactions between the nanoparticle ligands and the host domain. Finally, it mitigates entropic penalties associated with NP incorporation within the target domain of the BCP composite. This general approach provides a simple, efficient pathway for the fabrication of well-ordered organic/nanoparticle hybrid materials with the NP core content over 40 wt %.



INTRODUCTION

Polymer/inorganic hybrid materials with well-ordered structures have attracted enormous attention in recent years due to their many potential applications, including microelectronics, energy conversion, photonic devices, and sensors.^{1–12} The utility of these hybrid materials for a specific application is often dependent not only on the size, shape, and orientation of the ordered domains but also on the loading of the active nanoparticle (NP) constituent. Despite a significant amount of research,^{13–21} straightforward, general methods for achieving the latter goal are lacking.

The realization of ordered block copolymer/NP systems results from an energy balance between enthalpic and entropic contributions: the enthalpic contribution is controlled by the interaction between the additive and the block copolymer segments, while the entropic contribution arises in part from the chain stretching penalty for accommodating NPs.^{22,23} To date, most studies of NP incorporation in BCPs have involved NP ligands that are chemically identical to one of the blocks, yielding an enthalpically neutral interaction, or NP ligands that exhibit weak interactions with the target domain.^{13–21} In these cases, the entropic penalty for NP incorporation can easily dominate the system resulting in low NP loadings, particle aggregation/macrophase separation, or loss of order.

To achieve high loading of the NPs while maintaining ordered structures, the BCP/NP system needs to be optimized in order to either be enthalpically favorable or to reduce the

entropic penalties for NP incorporation. The Xu group²² took the latter approach to relieve entropic penalties in a composite system by introducing 3-*n*-pentadecylphenol or 4-(4'-octylphenyl)azophenol into poly(styrene-*block*-4-phenylpyridine) hosts for NPs functionalized with alkane ligands. The polar head groups of the additives hydrogen bond with the PVP block of the copolymer to supramolecular assemblies bearing alkane comb structures, which in turn interact with the alkane ligands of the NPs through dispersion interactions. While the NP ligand interactions with the polymer assemblies are weak, the creation of the comb structure, which contains many additional chain ends, reduces the entropic penalty for NP incorporation.

To date, surprisingly few studies^{23–27} have focused on the use of strong, favorable enthalpic interactions between the BCP and NP ligands to offset the entropic chain stretching penalty. The Wiesner group demonstrated coassembly of metal NPs coated with an organic shell composed of ionic liquid coatings and specially designed poly(isoprene-*block*-dimethylaminoethyl methacrylate) BCPs for the purpose of creating mesoporous metal assemblies;²⁴ however, their system employed very specific chemistries and cumbersome processing. More recently, our group developed an approach called additive-driven self-assembly^{28–30} to achieve strong microphase

Received: February 13, 2014

Published: February 25, 2014

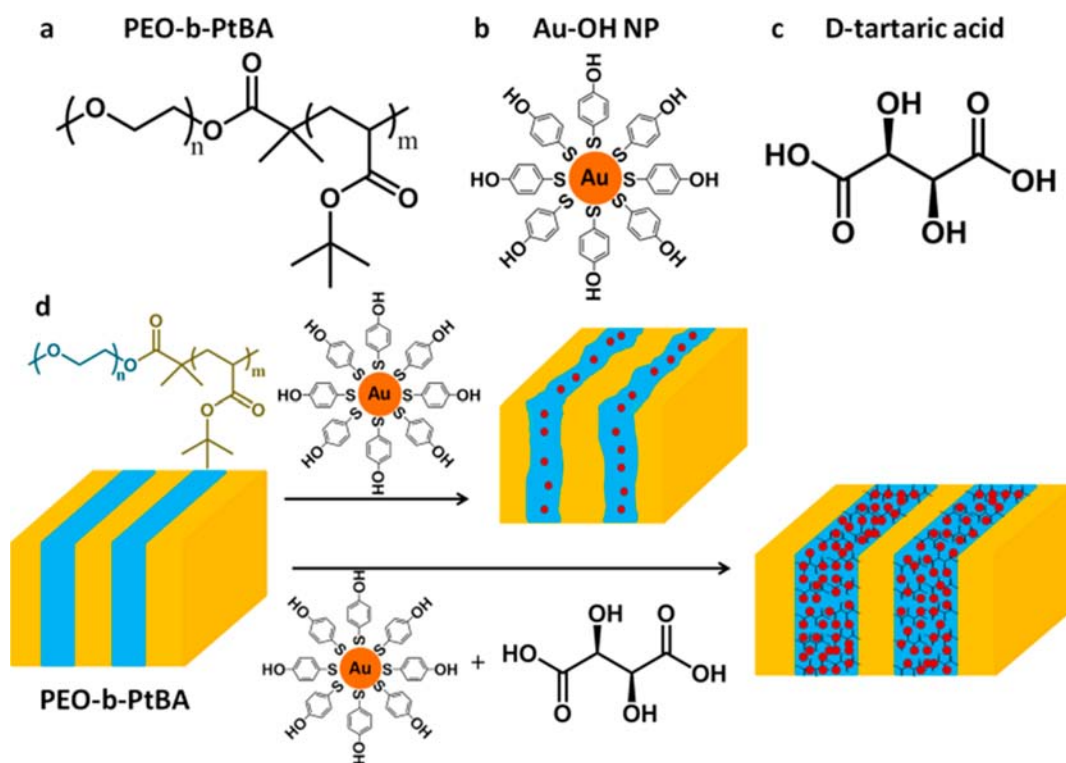


Figure 1. Structures of PEO-*b*-PtBA (a), Au-OH NPs with 4-hydroxythiophenol as ligands (b), and D-tartaric acid (c). (d) Schematic demonstration of PEO-*b*-PtBA blended with only Au-OH NPs and Au-OH NPs together with D-tartaric acid.

segregation in block copolymers that are otherwise disordered or weakly segregated by blending them with homopolymers,²⁹ small molecule additives,^{28,31} or nanoparticles.²³ We demonstrated that selective H-bonding interactions between the additives and one block of the block copolymer can effectively enhance the segregation strength of the system. This method offers a general approach to well-ordered polymer/NP composites by blending nanoparticles, which are functionalized with short H-bond-donating ligands, with block copolymers containing H-bond-accepting segments.²³ In one study we used 4-hydroxythiophenol-functionalized Au (Au-OH) NPs as the H-bond-donating additives and the PEO blocks of Pluronic surfactant block copolymers poly(ethylene oxide)-*block*-poly-(propylene oxide)-*block*-poly(ethylene oxide) (PEO-*b*-PPO-*b*-PEO) and poly(ethylene oxide)-*block*-polystyrene (PEO-*b*-PS) diblock copolymers as the H-bond-accepting segments. Well-ordered composites with Au-OH NP loadings of about 0.77 (weight ratio of Au NPs relative to PEO) were achieved using otherwise disordered or weakly segregated block copolymers hosts.

Here, we report a method for the ultrahigh loading of NPs in well-ordered block copolymer/additive systems through the consideration of both enthalpic and entropic factors. By incorporating small molecule additives (organic acids) that interact with both the NP ligand and one segment of the block copolymer host, the NP loading limit is dramatically increased. The role of the organic acid is threefold. First, it acts as an H-bond-donating additive to induce microphase separation in otherwise disordered or weakly segregated systems; the segregation strength of the block copolymer system is enhanced through the selective interaction of the acid with the PEO block. This interaction generates ordered structures in even low-molecular-weight systems. Additionally, the volume

fractions of the systems can be tuned by varying the acid loading, providing a facile means for achieving the desired morphology. Second, the acid can provide additional H-bond-accepting sites in a well-segregated amphiphilic system. The multiple carboxylic acid groups of the acid molecule make confinement of additional H-bond-donating NPs in the hydrophilic domain possible. The much stronger H-bonding interaction between carboxylic acid groups of the acid and the hydroxyl groups of the ligands of NPs enhances the favorable interaction between the NPs and hydrophilic domain. Third, the small additives in the PEO domain help alleviate the entropic penalties associated with NP incorporation by increasing the configurational entropy of the system by swelling of the BCP domains. In this context the tartaric acid plays the role of a selective solvent in a BCP composite system.³² Thus, ultrahigh metal content and precise particle distribution in the BCP system can be achieved with improved ordering.

EXPERIMENTAL SECTION

Materials. Poly(ethylene oxide-*b*-*tert*-butyl acrylate) (PEO-*b*-PtBA) diblock copolymer was synthesized using atom transfer radical polymerization (ATRP) following the established procedures,³³ with slight modifications; D-tartaric acid was purchased from Sigma-Aldrich; Au-OH nanoparticles (NPs) with the diameter of 2–3 nm functionalized with 4-hydroxythiophenol were synthesized following the established procedures.³⁴ Ruthenium tetroxide (RuO₄) 0.5 wt % aqueous solution was purchased from Electron Microscopy Sciences.

Sample Preparation and Characterization. Preparation of bulk samples for small-angle X-ray. PEO-*b*-PtBA, D-tartaric acid, and Au-OH NPs were blended at a given mass ratio in dimethylformamide (DMF) of a certain weight percentage (BCP concentration of 2–3 wt %). After dropped cast from the DMF solution onto glass slides, dried at room temperature (rt), annealed for 36 h at 90 °C under vacuum, and then cooled to rt under vacuum, the bulk samples were scraped off

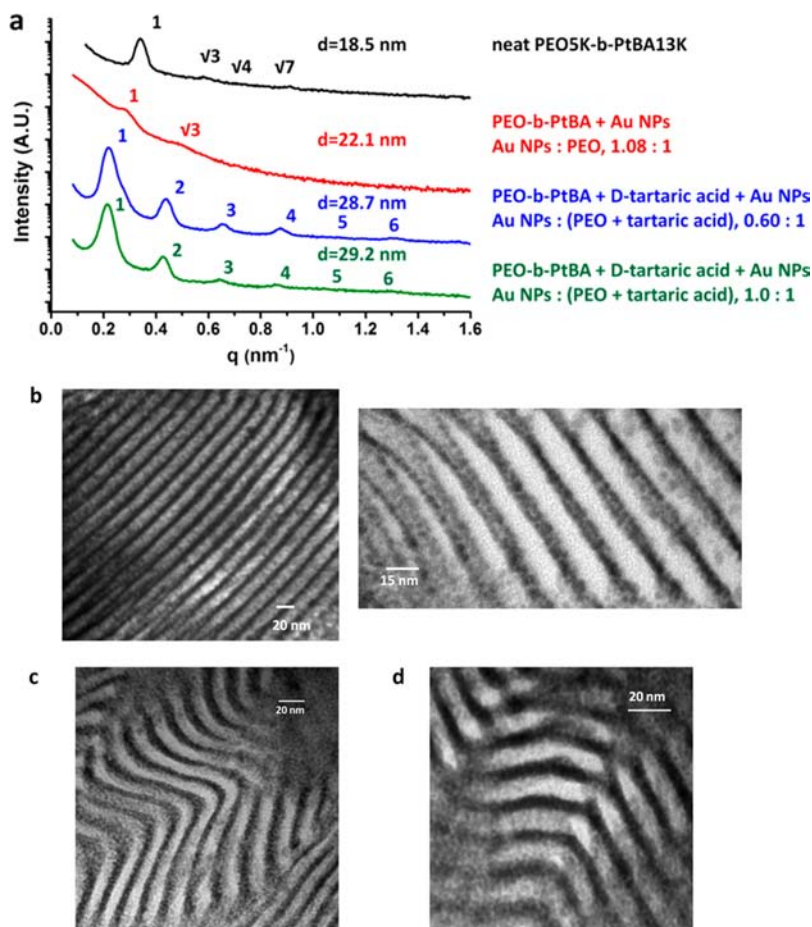


Figure 2. (a) SAXS profiles of neat PEO-*b*-PtBA (18K, 72.3 wt % PtBA, PDI = 1.12); PEO-*b*-PtBA blended with Au-OH NPs (Au NPs: PEO, 1.08:1); PEO-*b*-PtBA + D-tartaric acid (PEO:tartaric acid, 56:44) blended with Au-OH NPs (Au NPs:(PEO + tartaric acid), 0.60:1); PEO-*b*-PtBA + D-tartaric acid (PEO:tartaric acid, 56:44) blended with Au-OH NPs (Au NPs:(PEO + tartaric acid), 1:1). (b–d) TEM images of PEO-*b*-PtBA (18K, 72.3 wt % PtBA, PDI = 1.12) + D-tartaric acid (PEO:tartaric acid, 56:44) blended with Au NPs (Au NPs:(PEO + tartaric acid), 0.60:1), after cryo-microtoming without staining (b), with RuO₄ staining for 3 min (c), and with RuO₄ staining for 10 min (d).

the glass slides and then evenly placed in the center of metal washers sandwiched by Kapton film.

Small-angle X-ray scattering (SAXS). The samples were placed on a heated vertical holder which was equilibrated at 90 °C for about 20 min under vacuum. The whole system was under vacuum during the measurements which were done at UMass Amherst using an in-house setup from Molecular Metrology Inc. (presently sold as Rigaku S-Max3000) with the wavelength of 0.1542 nm and sample-to-detector distance of 1477 mm.

Transmission electron microscopy (TEM). Cryo-microtoming was used to cut the bulk sample into pieces with the thickness of 50 nm, which is thin enough for electron beam going through, with the cutting atmosphere temperature of –120 °C and knife temperature of –110 °C below the glass transition temperature (T_g) of PEO block. A JEOL 2000FX electron microscope which was operating at 200 kV was used. The samples are either without any staining or stained using ruthenium tetroxide (RuO₄) with the vapor concentration of 2 mL 0.5 wt % aqueous solution in a 250 mL jar for 3 and 10 min.

Thermogravimetric analysis (TGA) was performed on a TGA 500 thermogravimetric analyzer heating at a rate of 10 °C/min from room temperature to 800 °C under a continuous purge of nitrogen.

RESULTS AND DISCUSSION

We used enantiopure tartaric acid, which was used in our previous studies of disordering transitions for hierarchical pattern formation, as the organic acid additive.³⁵ Tartaric acid is a chiral acid that contains two stereocenters in its backbone as

well as multiple H-bond-donating and H-bond-accepting groups, including carboxylic acid and hydroxyl groups as shown in Figure 1c. Here, enantiopure D-tartaric acid was used rather than racemic tartaric acid because the enantiomers in the racemic mixture interact more strongly with each other than they do with the ether groups of the PEO block.³⁵ We used poly(ethylene oxide-*block-tert*-butyl acrylate) PEO-*b*-PtBA (Figure 1a) as the BCP host and gold NPs functionalized with 4-hydroxythiophenol (Au-OH) as the nanoparticle additives (Figure 1b). In Figure 1d, we illustrate that blending D-tartaric acid into the PEO-*b*-PtBA BCP system creates additional H-bond-accepting groups in the hydrophilic PEO domain.

For consistency, we express the composition of the hydrophilic domain (PEO:tartaric acid) as the mass ratio of PEO to tartaric acid. We express loadings of Au NPs within composites by the mass ratio of Au NPs to either neat PEO block or the PEO block plus tartaric acid. These are denoted as Au NPs:PEO or Au NPs:(PEO + tartaric acid). Thermogravimetric analysis (TGA) indicated that the Au-OH NPs used in this study contain ~72% Au by weight; the balance is ligand.²³ Using this information, Au loadings relative to a variety of basis can be calculated. We use TGA to verify these calculations by computing the Au mass fractions of the ordered composites (vide infra).

PEO-*b*-PtBA BCP with a molecular weight of 18K, 72.3 wt % PtBA, and PDI of 1.12 (denoted as PEO5K-*b*-PtBA13K) was used as the host. Au (Au-OH) NPs with the diameters of ca. 2–3 nm functionalized with 4-hydroxythiophenol were synthesized using the same procedure as our previous study²³ following the literature procedures with slight modification.³⁴ The small-angle X-ray scattering (SAXS) profile for neat PEO5K-*b*-PtBA13K is shown in Figure 2a, and the higher order reflections indicate an ordered cylindrical morphology, with a *d*-spacing of 18.5 nm. By blending Au-OH NPs (Au NPs:PEO, 1.08:1) into PEO5K-*b*-PtBA13K, the *d*-spacing was increased from 18.5 to 22.1 nm. However, the scattering peaks were heavily attenuated with a large increase in the full width at half-maximum intensity, indicating disordered phase due to significant weakening in the strength of segregation and possible nanoparticle macrophase segregation. The loss in intensity occurs despite an expected increase in the electron density contrast of the two domains. By contrast, the addition of D-tartaric acid (PEO:tartaric acid, 56:44) into the system with the same amount of Au NPs (Au NPs:PEO, 1.08:1 or Au NPs:(PEO + tartaric acid), 0.60:1) yielded well-defined scattering peaks (Figure 2a), revealing a lamellar morphology as indicated by the ratios of the multiple higher-order peaks to the primary peak (1:2:3:4:5:6) and a *d*-spacing of 28.7 nm. The well-resolved higher-order peaks confirm the excellent ordering with good electron density contrast between the two domains, indicating that the NPs were selectively confined to one domain. Not surprisingly, the ultrahigh loading of the additives changes the volume fraction of the system and can lead transitions between ordered morphologies. We further demonstrated that Au-OH NPs with the amount as high as 1:1 (Au NPs:(PEO + tartaric acid)) can be loaded in PEO5K-*b*-PtBA13K as shown in Figure 2a.

Transmission electron microscopy (TEM) was used to characterize the detailed structure of the system and to confirm the location of the NPs. The TEM images in Figure 2b show the well-ordered lamellar morphology of the sample without any staining. Individual nanoparticles that are densely packed and confined in one domain are clearly resolved in the image. Ruthenium tetroxide (RuO₄) vapor (2 mL 0.5 wt % solution in a 250 mL jar) was used to stain the PEO domain (Figure 2c,d). The clear contrast in both TEM images helps confirm that the nanoparticles were confined solely to the PEO domain.

To achieve ultrahigh Au content of the composite system, we used a PEO-*b*-PtBA BCP with higher PEO volume fraction as the loading substrate. The molecular weight of the PtBA block in the new copolymer (denoted as PEO5K-*b*-PtBA4.2K) with a PDI of 1.04 was reduced to 4.2K (from 13K) while the molecular weight of the PEO block was maintained at 5K. D-tartaric acid (PEO:tartaric acid, 58:42) was added into the system to allow for the ultrahigh loading of NPs. Both TEM and SAXS were again used to confirm the loading of Au-OH nanoparticles. As shown in Figure 3a, ordered lamellar morphology was observed in TEM for the sample with Au-OH NPs loading amount as high as 1.07:1 (Au NPs:(PEO + tartaric acid)). The SAXS profiles in Figure 3b show that ordering peaks were clearly observed even with the Au-OH NPs were added at a loading of 1.50:1 (Au NPs:(PEO + tartaric acid)). A meaningful comparison to NP loadings in our previous study requires consideration of NP loading with respect to the both PEO mass in the copolymer and the total mass of the target domain, which includes tartaric acid in the present study. The weight ratio of Au-OH NPs to PEO block is

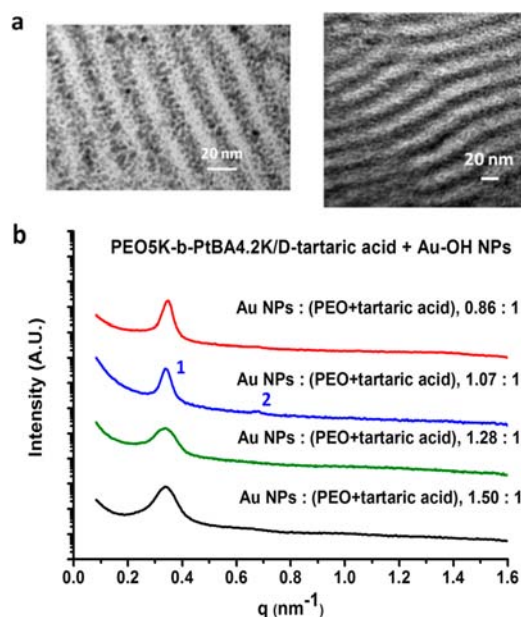


Figure 3. (a) TEM images of PEO-*b*-PtBA (9.2K, 46.6 wt % PtBA, PDI = 1.04) + D-tartaric acid (PEO:tartaric acid, 58:42) blended with Au-OH NPs (Au NPs:(PEO + tartaric acid), 1.07:1). (b) SAXS profiles of PEO-*b*-PtBA + D-tartaric acid (PEO:tartaric acid, 58:42) blended with different amounts of Au-OH NPs (Au NPs:(PEO + tartaric acid), 0.86:1, 1.07:1, 1.28:1, and 1.50:1).

up to 2.63 in this study compared to 0.77 in the previous study. When normalized for the mass of all organic compounds in hydrophilic domain (PEO plus D-tartaric acid if any), the ratio is up to 1.5 for this study, nearly twice the ratio of 0.77 achieved in our previous study.

TGA was used to confirm inorganic content in the system. The Au content in the Au-OH NPs used here is ~ 72 wt %.²³ With Au-OH NP, 0.86 of Au NPs:(PEO + tartaric acid), loaded into a PEO5K-*b*-PtBA4.2K/D-tartaric acid (PEO:tartaric acid, 58:42) composite system, the calculated Au content of the total compound is 26%. The experimental result from TGA in Figure 4a showed that the inorganic compounds that remained after heating to 800 °C made up $\sim 28\%$ of the compound. With Au-OH NPs (Au NPs:(PEO + tartaric acid), 1.28:1) loaded, the calculated Au content should be 39%, while the experimental result from TGA in Figure 4b gave the percentage of inorganic compounds left to be about 42%. A control experiment in Figure 4c shows that about 3% of the neat PEO5K-*b*-PtBA4.2K/D-tartaric acid composite (PEO:tartaric acid, 58:42) is left after heating without any NP loading due to the carbonization of the organic compounds in the system. After subtracting the carbonization residue in each case, all the experimental Au-OH contents match well with the calculated results.

To further illustrate the concept, we studied morphology and *d*-spacing development in the PEO-*b*-PtBA composite system through the comparison of neat PEO-*b*-PtBA, PEO-*b*-PtBA blended with only D-tartaric acid, and PEO-*b*-PtBA blended with both D-tartaric acid and Au-OH NPs. The SAXS profiles in Figure 5 show that ordering was dramatically improved after blending D-tartaric acid (PEO:tartaric acid, 58:42) into the neat PEO-*b*-PtBA (PEO5K-*b*-PtBA4.2K). The ratios of ordering peaks to the primary peak are 1:2:3:4, indicating lamellar morphology. The *d*-spacing was also dramatically increased from 12.7 to 17.5 nm. DSC and WAXS studies in our previous

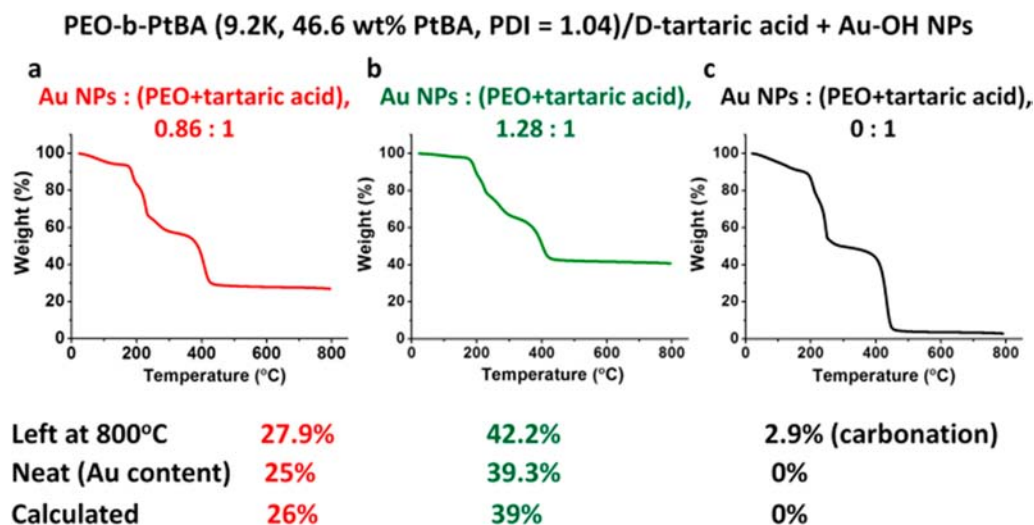


Figure 4. TGA of PEO-*b*-PtBA (9.2K, 46.6 wt % PtBA, PDI = 1.04) + D-tartaric acid (PEO:tartaric acid, 58:42) blended with different amounts of Au-OH NPs (Au NPs:(PEO + tartaric acid), 0.86:1 (a), 1.28:1 (b), 0:1 (c)). For (a) 27.9% remaining after 800 °C with 25% Au (measured), 26% Au (calculated); for (b) 42.2% remaining after 800 °C with 39.3% Au (measured), 39% Au (calculated); for (c) 2.9% remaining after 800 °C, 0% Au (measured), 0% Au (calculated).

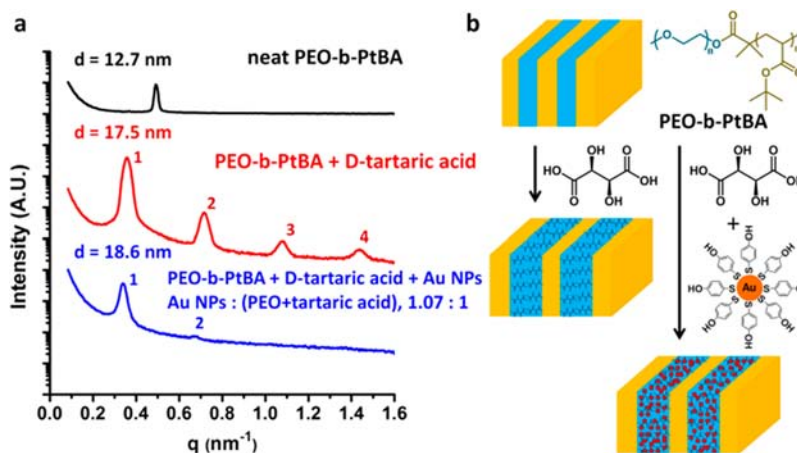


Figure 5. (a) SAXS profiles of neat PEO-*b*-PtBA (9.2K, 46.6 wt % PtBA, PDI = 1.04); PEO-*b*-PtBA + D-tartaric acid (PEO:tartaric acid, 58:42); PEO-*b*-PtBA + D-tartaric acid (PEO:tartaric acid, 58:42) blended with Au-OH NPs (Au NPs:(PEO + tartaric acid), 1.07:1). (b) Schematic representation of PEO-*b*-PtBA blended only with D-tartaric acid and D-tartaric acid together with Au-OH NPs.

work³⁵ showed that the interaction between D-tartaric acid and PEO domain was strong enough to inhibit the crystallization of PEO, indicating that the D-tartaric acid resided in the PEO domain. By blending an additional Au-OH NPs with the loading amount, 1.07:1 (Au NPs:(PEO + tartaric acid)), into the system, the *d*-spacing increased to 18.6 nm.

CONCLUSIONS

We have demonstrated a simple and efficient pathway for the fabrication of well-ordered organic/metal hybrid materials with ultrahigh NP content. Introduction of small molecule additives that hydrogen bond with the nanoparticle ligands and one segment of the block copolymer host enables high loading of NPs in well-ordered composites through the introduction of favorable enthalpic interactions, increases in segregation strength and mitigation of entropic penalties for NP incorporation. High NP loading is essential for many applications of ordered polymer/NP composites. We further note that this method provides advantages for the practical

fabrication of well-ordered functional hybrid nanomaterials via large-scale manufacturing (e.g., roll-to-roll coating).

ASSOCIATED CONTENT

Supporting Information

SAXS of PEO-*b*-PtBA (18K, 72.3 wt % PtBA, PDI of 1.12)/D-tartaric acid (PEO:D-tartaric acid, 56:44) blended with Au-OH NPs (Au NPs:(PEO + tartaric acid), 0.2:1, 0.6:1, 0.8:1, and 1:1). This material is available free of charge via the Internet at <http://pubs.acs.org>.

AUTHOR INFORMATION

Corresponding Author

*E-mail: watkins@polysci.umass.edu (J.J.W.).

Notes

The authors declare no competing financial interest.

ACKNOWLEDGMENTS

This work was supported by the NSF Center for Hierarchical Manufacturing at University of Massachusetts Amherst

(CMMI-1025020). Facilities used in this work were supported by the Materials Research Science and Engineering Center at University of Massachusetts Amherst. We thank Nichalos Colella, Cheng Li, and Dr. Vikram Daga for helpful discussions.

REFERENCES

- (1) Boal, A. K.; Ilhan, F.; DeRouchey, J. E.; Thurn-Albrecht, T.; Russell, T. P.; Rotello, V. M. *Nature* **2000**, *404*, 746–748.
- (2) Huynh, W. U.; Dittmer, J. J.; Alivisatos, A. P. *Science* **2002**, *295*, 2425–2427.
- (3) Balazs, A. C.; Emrick, T.; Russell, T. P. *Science* **2006**, *314*, 1107–1110.
- (4) Rancatore, B. J.; Mauldin, C. E.; Tung, S.-H.; Wang, C.; Hexemer, A.; Strzalka, J.; Fréchet, J. M. J.; Xu, T. *ACS Nano* **2010**, *4*, 2721–2729.
- (5) Lopes, W. A.; Jaeger, H. M. *Nature* **2001**, *414*, 735–738.
- (6) Rosa, C. D.; Auriemma, F.; Girolamo, R. D.; Pepe, G. P.; Napolitano, T.; Scaldasferri, R. *Adv. Mater.* **2010**, *22*, 5414–5419.
- (7) Lin, Y.; Wei, Q.; Qian, G.; Yao, L.; Watkins, J. J. *Macromolecules* **2012**, *45*, 8665–8673.
- (8) Wei, Q.; Lin, Y.; Anderson, E. R.; Briseno, A. L.; Gido, S. P.; Watkins, J. J. *ACS Nano* **2012**, *6*, 1188–1194.
- (9) Lu, G.; Li, L.; Yang, X. *Small* **2008**, *4*, 601–606.
- (10) Kim, H.; Kobayashi, S.; AbdurRahim, M. A.; Zhang, M. J.; Khusainova, A.; Hillmyer, M. A.; Abdala, A. A.; Macosko, C. W. *Polymer* **2011**, *52*, 1837–1846.
- (11) Zhang, K.; Wang, Y.; Hillmyer, M. A.; Francis, L. F. *Biomaterials* **2004**, *25*, 2489–2500.
- (12) Cushen, J. D.; Otsuka, I.; Bates, C. M.; Halila, S.; Fort, S.; Rochas, C.; Easley, J. A.; Rausch, E. L.; Thio, A.; Borsali, R.; Willson, C. G.; Ellison, C. J. *ACS Nano* **2012**, *6*, 3424–3433.
- (13) Gaines, M. K.; Smith, S. D.; Samseth, J.; Bockstaller, M. R.; Thompson, R. B.; Rasmussen, K. O.; Spontak, R. J. *Soft Matter* **2008**, *4*, 1609–1612.
- (14) Kim, B. J.; Chiu, J. J.; Yi, G. R.; Pine, D. J.; Kramer, E. J. *Adv. Mater.* **2005**, *17*, 2618–2622.
- (15) Kang, H.; Detcheverry, F. A.; Mangham, A. N.; Stoykovich, M. P.; Daoulas, K. C.; Hamers, R. J.; Müller, M.; de Pablo, J. J.; Nealey, P. F. *Phys. Rev. Lett.* **2008**, *100*, 148303.
- (16) Chiu, J. J.; Kim, B. J.; Kramer, E. J.; Pine, D. J. *J. Am. Chem. Soc.* **2005**, *127*, 5036–5037.
- (17) Costanzo, P. J.; Beyer, F. L. *Macromolecules* **2007**, *40*, 3996–4001.
- (18) Chiu, J. J.; Kim, B. J.; Yi, G.-R.; Bang, J.; Kramer, E. J.; Pine, D. J. *Macromolecules* **2007**, *40*, 3361–3365.
- (19) Matsen, M. W.; Thompson, R. B. *Macromolecules* **2008**, *41*, 1853–1860.
- (20) Zou, S.; Hong, R.; Emrick, T.; Walker, G. C. *Langmuir* **2007**, *23*, 1612–1614.
- (21) Kim, B. J.; Bang, J.; Hawker, C. J.; Kramer, E. J. *Macromolecules* **2006**, *39*, 4108–4114.
- (22) Zhao, Y.; Thorkeleson, K.; Mastroianni, A. J.; Schilling, T.; Luther, J. M.; Rancatore, B. J.; Matsunaga, K.; Jinnai, H.; Wu, Y.; Poulsen, D.; Frechet, J. M. J.; Paul Alivisatos, A.; Xu, T. *Nat. Mater.* **2009**, *8*, 979–985.
- (23) Lin, Y.; Daga, V. K.; Anderson, E. R.; Gido, S. P.; Watkins, J. J. *J. Am. Chem. Soc.* **2011**, *133*, 6513–6516.
- (24) Warren, S. C.; Messina, L. C.; Slaughter, L. S.; Kamperman, M.; Zhou, Q.; Gruner, S. M.; DiSalvo, F. J.; Wiesner, U. *Science* **2008**, *320*, 1748–1752.
- (25) Noro, A.; Higuchi, K.; Sageshima, Y.; Matsushita, Y. *Macromolecules* **2012**, *45*, 8013–8020.
- (26) Jang, S. G.; Khan, A.; Hawker, C. J.; Kramer, E. J. *Macromolecules* **2012**, *45*, 1553–1561.
- (27) Jang, S. G.; Kramer, E. J.; Hawker, C. J. *J. Am. Chem. Soc.* **2011**, *133*, 16986–16996.
- (28) Daga, V. K.; Watkins, J. J. *Macromolecules* **2010**, *43*, 9990–9997.
- (29) Tirumala, V. R.; Daga, V.; Bosse, A. W.; Romang, A.; Ilavsky, J.; Lin, E. K.; Watkins, J. J. *Macromolecules* **2008**, *41*, 7978–7985.
- (30) Tirumala, V. R.; Romang, A.; Agarwal, S.; Lin, E. K.; Watkins, J. J. *Adv. Mater.* **2008**, *20*, 1603–1608.
- (31) Daga, V. K.; Anderson, E. R.; Gido, S. P.; Watkins, J. J. *Macromolecules* **2011**, *44*, 6793–6799.
- (32) Sarkar, B.; Alexandridis, P. *Langmuir* **2012**, *28*, 15975–15986.
- (33) Davis, K. A.; Charleux, B.; Matyjaszewski, K. J. *Polym. Sci., Part A: Polym. Chem.* **2000**, *38*, 2274–2283.
- (34) Brust, M.; Fink, J.; Bethell, D.; Schiffrin, D. J.; Kiely, C. *Chem. Commun.* **1995**, 1655–1656.
- (35) Yao, L.; Watkins, J. J. *ACS Nano* **2013**, *7*, 1513–1523.